The EMBO Journal Vol. 22 No. 2 pp. 236–245, 2003

Heparan sulfate chains of perlecan are indispensable in the lens capsule but not in the kidney

Maarit Rossi[1], Hiroyuki Morita[2], Raija Sormunen[3], Sari Airenne[4], Marjut Kreivi[1], Ling Wang[2], Naomi Fukai[5], Bjorn R.Olsen[5], Karl Tryggvason[2] and Raija Soininen[1,2,6]

Biocenter Oulu, [1]Department of Medical Biochemistry and Molecular Biology, [3]Department of Pathology, [4]Department of Biochemistry, University of Oulu, FIN-90014 Oulu, Finland, [2]Division of Matrix Biology, Department of Medical Biochemistry and Biophysics, Karolinska Institutet, S-171 77 Stockholm, Sweden and [5]Department of Cell Biology, Harvard Medical School, Boston, MA 02115, USA

[6]Corresponding author
e-mail: raija.soininen@oulu.fi

Mice lacking exon 3 of perlecan (*Hspg2*) gene were generated by gene targeting. Exon deletion does not alter the expression or the reading frame but causes loss of attachment sites for three heparan sulfate (HS) side chains. *Hspg2*$^{\Delta3/\Delta3}$ mice are viable and fertile but have small eyes. Apoptosis and leakage of cellular material through the lens capsule are observed in neonatal lenses, and lenses degenerate within 3 weeks of birth. Electron microscopy revealed altered structure of the lens capsule through which cells had formed extensions. No kidney malfunction, such as proteinuria, was detected in *Hspg2*$^{\Delta3/\Delta3}$ mutant mice, nor were ultrastructural changes observed in the glomerular basement membranes (BMs). To achieve further depletion in the HS content of the BMs, *Hspg2*$^{\Delta3/\Delta3}$ mice were bred with collagen XVIII null mice. Lens defects were more severe in the newborn *Col18a1*$^{-/-}$ × *Hspg2*$^{\Delta3/\Delta3}$ mice and degeneration proceeded faster than in *Hspg2*$^{\Delta3/\Delta3}$ mice. The results suggest that in the lens capsule, HS chains have a structural function and are essential in the insulation of the lens from its environment and in regulation of incoming signals.

Keywords: basement membranes/collagen XVIII/congenital cataract/heparan sulfate/perlecan

Introduction

Heparan sulfate proteoglycans (HSPG) are composed of a core protein and heparan sulfate (HS) side chains attached to it. HS chains are unbranched polysaccharide chains composed of repeating disaccharide units that are sulphated and negatively charged. HSs are highly hydrophilic and can form gels of varying pore size and charge density. HSPGs in the extracellular matrix bind growth factors thus forming a growth factor reservoir, protect growth factors from degradation and regulate their transport and accessibility (Iozzo, 1998). The presence of HS in basement membranes (BMs) was first detected in glomerular BM (Kanwar and Farquhar, 1979), and it was suggested that these polymers establish the permeability barrier for macromolecules.

Perlecan is a large multidomain HS proteoglycan found in all BMs, and also in the tissue stroma of liver and in cartilage where no BM is present (Iozzo *et al*., 1994). Perlecan is tightly bound to other matrix components and can self-assemble into dimers and larger aggregates (Yurchenco *et al*., 1987). The murine perlecan core protein has five distinct domains, the sequence motifs of which resemble the domains of the laminin α1 chain, low density lipoprotein receptor, and N-CAM (Noonan *et al*., 1991), and has an estimated size of 390 kDa, while the fully glycosylated protein is ~700 kDa (Hassell *et al*., 1980). Three large HS chains extend from one end of the core protein as detected by rotary shadowing (Paulsson *et al*., 1987), and the attachment sites for these side chains have been localized to conserved serine residues 65, 71 and 76 in the N-terminal domain I (Noonan *et al*., 1991; Kallunki and Tryggvason, 1992; Dolan *et al*., 1997). An additional substitution site for an HS chain has been localized to domain V (Friedrich *et al*., 1999; Tapanadechopone *et al*., 1999). Thus, up to four HS chains can be attached to the perlecan core protein. Chondroitin sulfate/dermatan sulfate chains occasionally replace HS chains in perlecan, and a portion of the secreted perlecan can be totally devoid of glycosaminoglycan side chains (Iozzo, 1998).

Perlecan has been described as a low affinity FGF-2 coreceptor, an inducer for high affinity binding of FGF-2 (Aviezer *et al*., 1994), and FGF-2 binding has been localized to the HS chains located in domain I in the perlecan core protein (Whitelock *et al*., 1996). As a major BM HSPG, perlecan has been thought to have a crucial role in the filtration barrier formation in the glomerular BM. Furthermore, the HS chains of perlecan have been shown to have a role in the regulation of cell adhesion to the substrate. Endothelial cells adhere to the perlecan core protein through β1 and β3 integrins, and the adhesion is inhibited by HS (Hayashi *et al*., 1992). The adhesion of smooth muscle cells to fibronectin is inhibited by perlecan, and the anti-adhesive effect is reduced by heparinase treatment (Lundmark *et al*., 2001). On the other hand, heparitinase treatment reduced cell attachment to perlecan when various cell lines were studied, and it was suggested that cooperation between the core protein and HS chains is required for cell attachment (Battaglia *et al*., 1993). Both HS chains and specific domains in the core protein are involved in the interactions of perlecan with other BM components so that laminin and collagen IV bind to perlecan mainly through the HS chains, whereas nidogen mainly binds to the perlecan core protein (Battaglia *et al*., 1992; Timpl and Brown, 1996).

Perlecan null mice die during embryogenesis or as neonates. Inactivation of the perlecan gene has a major effect on the development of cartilage, so that the cartilage matrix is disorganized and chondrocyte proliferation is reduced (Arikawa-Hirasawa *et al*., 1999; Costell *et al*., 1999). Formation of BMs proceeds normally, but mechanical stress causes their disruption in expanding brain vesicles and contracting myocardium (Costell *et al*., 1999), indicating loss of tensile strength.

Perlecan contains significant amounts of negatively charged HS, but there is still little knowledge about the specific biological roles of this HS, the major proportion of which is present in three large N-terminal side chains. We were interested in the functions of perlecan HS *in vivo*, especially with respect to its potential role in the renal filtration barrier. In order to address these questions, we generated mice in which most, if not all, of the HS chains are eliminated, while the core protein is produced normally. The resulting mice with HS-depleted perlecan are viable, but their lenses deteriorate early. Perhaps surprisingly, the kidney function is not affected.

Two additional BM components, agrin (Tsen *et al*., 1995) and collagen XVIII (Halfter *et al*., 1998) have been shown to carry HS chains. To further analyze the significance of HS in BMs, we bred mice with the HS-depleted perlecan with collagen XVIII null mice (Fukai *et al*., 2002). *Col18a1*$^{-/-}$ mice have normal lenses, but in the double mutant mice, lens degeneration appears earlier than in mice carrying perlecan mutation alone, implying that HS chains of different lens capsule components can substitute for each other to some extent, and are essential for the function and postnatal development of the lens.

Results

Targeted alteration of the perlecan gene and characterization of the gene product

The HS attachment sites were abolished by targeted deletion of exon 3 in the perlecan (*Hspg2*) gene in embryonic stem (ES) cells. The targeting vector contained 7.5 kb of genomic DNA in which a 130 bp fragment containing exon 3 and the surrounding intron sequences was replaced by the neomycin resistance gene, driven by the PGK promoter (Figure 1A). The codons are split after the first nucleotide at the 3′ end in both exons 2 and 3 (Cohen *et al*., 1993), therefore, deletion of exon 3 does not alter the reading frame in the perlecan mRNA. Exon 3 is 45 bp in size and codes for two Ser–Gly–Asp triplets, where the serine is the residue for the attachment of a HS chain. The codon for aspartate in the extreme N-terminal Ser–Gly–Asp triplet is split between exons 2 and 3 and is lost when exon 3 is deleted, which is likely to lead to the abolishment of this HS attachment site too.

The linearized targeting construct DNA was electroporated into the ES cells. Cells were selected in G418, clones carrying the targeted mutation were identified by Southern analysis (Figure 1B) and injected into C57BL/6 blastocysts. Germline transmission was obtained from two ES cell clones. No difference in viability, growth or fertility was observed between homozygous *Hspg2*$^{\Delta3/\Delta3}$ mutant, heterozygous and wild-type mice.

To verify that splicing of the perlecan mRNA had occurred as predicted, RT–PCR was performed with

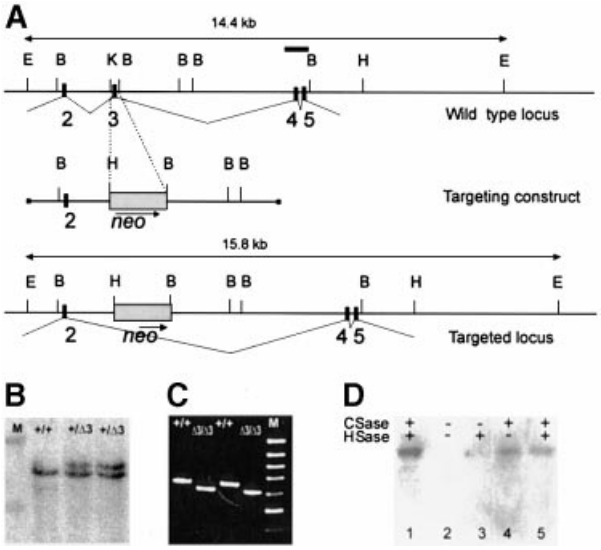

Fig. 1. Deletion of exon 3 in the perlecan (*Hspg2*) gene. (**A**) Region of the perlecan gene containing exons 2–5 (top), the targeting construct (middle) and the region after homologous recombination. Exons are depicted as black boxes and numbered. A 130 bp *Kpn*I–*Bam*HI fragment containing exon 3 was replaced by the PGK-*neo* selection cassette. The probe containing exons 4 and 5 that was used for Southern blots is depicted as a bar (top). E, *Eco*RI; B, *Bam*HI; H, *Hin*dIII; K, *Kpn*I. (**B**) Southern blot analysis of *Eco*RI-digested DNA from ES cell clones. M, λ DNA digested with *Hin*dIII, upper band 19.9 kb, lower band 9.5 kb. (**C**) Products of RT–PCR reactions performed with primers coding for the N-terminal region of the perlecan protein (for sequences, see text) separated in an agarose gel. Sources of RNA were whole E16 embryos and primary fibroblasts isolated from newborn wild-type(+/+) or *Hspg2*$^{\Delta3/\Delta3}$ mice. M, 100 bp ladder, uppermost band 1000 bp. The PCR products are 650 bp in wild-type and 605 bp in mutant samples. (**D**) Immunoblot analysis of proteoglycan-enriched fractions isolated from the culture medium of wild-type and *Hspg2*$^{\Delta3/\Delta3}$ fibroblasts. Samples were treated with (+) or without (–) chondroitinase (CSase) and heparitinase (HSase), subjected to SDS–PAGE in a 5% gel, and resolved by immunoblotting with an antibody against perlecan. Lane 1, wild-type sample treated with chondroitinase and heparitinase; lane 2, untreated mutant sample; lane 3, mutant sample treated with heparitinase only; lane 4, mutant sample treated with chondroitinase only; lane 5, mutant sample treated with chondroitinase and heparitinase. The perlecan core protein produced by the mutant cells was of the same size as the wild-type perlecan, and core protein was observed after chondroitinase treatment, indicating that the major portion of the mutant perlecan carries chondroitin sulfate chains only.

primers coding for the N-terminal region of the protein using RNA isolated from wild-type and targeted ES cells, mouse embryos and from primary fibroblasts. The results showed the expected deletion of 45 bp in the PCR product originating from the *Hspg2*$^{\Delta3/\Delta3}$ mutant RNA (Figure 1C).

Proteoglycans isolated from the culture media of wild-type and *Hspg2*$^{\Delta3/\Delta3}$ mutant fibroblasts were treated with heparitinase and chondroitinase, and analyzed by SDS–PAGE and immunoblotting with anti-perlecan antibody. As expected, the perlecan core protein was the same size in wild-type and mutant samples after treatment with heparitinase and chondroitinase (Figure 1D). The untreated sample did not enter the gel and no band was visible, but perlecan isolated from *Hspg2*$^{\Delta3/\Delta3}$ mutant fibroblast medium and treated with chondroitinase alone did yield a clear band corresponding to the full-size core protein, whereas in the sample treated with heparitinase alone the band was hardly visible. These results demon-

Table I. Eye weights (mg) of wild-type and $Hspg2^{\Delta3/\Delta3}$ mutant mice

Age	Wild type	$Hspg2^{\Delta3/\Delta3}$ mutant	% of the wild type
Newborn	3.5 (10)	2.7 (10)	77.6
1 week	10.7 (10)	7.8 (10)	72.6
2 weeks	13.8 (10)	10.3 (10)	74.8
3 weeks	15.2 (10)	10.4 (10)	68.4
6–7 weeks	18.7 (12)	11.5 (10)	61.5
4 months	26.4 (10)	14.9 (10)	56.4
9 months	28.4 (11)	15.5 (12)	54.5
12 months	28.0 (3)	13.0 (6)	46.4

In parentheses, the number of eyes weighed.

strate that $Hspg2^{\Delta3/\Delta3}$ mutant fibroblasts produce perlecan core protein, and that the perlecan present in their medium mainly carries chondroitin sulfate, and only a small amount of HS.

Kidneys of the $Hspg2^{\Delta3/\Delta3}$ mice are not affected

Since HS depletion from perlecan was predicted to have a major effect on filtration in the kidney, urine samples from wild-type and $Hspg2^{\Delta3/\Delta3}$ mutant mice aged 6–8 weeks and 12–18 months were analyzed for the presence of protein. SDS–PAGE analysis did not demonstrate any increase in the protein content in the urine of $Hspg2^{\Delta3/\Delta3}$ mutant mice (data not shown), nor did they exhibit any manifestations of kidney dysfunction. Furthermore, no alterations in kidney morphology were observed in light microscopy, nor any alterations in the ultrastructure of the GBM of mutant mice in electron microscopy, even at the age of 18 months (data not shown).

Congenital cataract and microphthalmia in $Hspg2^{\Delta3/\Delta3}$ mutant mice

A major defect observed in the $Hspg2^{\Delta3/\Delta3}$ mutant mice is degeneration of lens at an early age. Lens degeneration is observed in all $Hspg2^{\Delta3/\Delta3}$ mutant mice, but never in heterozygotes or wild-type littermates, although eye defects of other kinds are occasionally detected in C57BL/6 mice. The gross morphology of the eyes is normal in newborn $Hspg2^{\Delta3/\Delta3}$ mutant mice, but the eyes are smaller, about 77% of the weight of wild-type mice of the same body weight. Eye weight increases in both wild-type and mutant mice as they grow, but the size difference increases with age (Table I). The lenses in newborn $Hspg2^{\Delta3/\Delta3}$ mutant mice appear, by light microscopy, well developed with the epithelial cells in the anterior region forming a single layer, and show the occurrence of normal proliferation and differentiation zones. The formation and organization of fiber cells, as well as the anterior and posterior sutures show no differences to the structure of wild-type lenses (Figure 2A). However, drops of foreign material are often seen in the vitreous chamber of $Hspg2^{\Delta3/\Delta3}$ mutant eyes, even in newborn mice. These drops can be traced to small leaks in the lens capsule in the lateral and posterior regions of the lens, and staining with γ crystallin antibodies verified that the material originates in the lens fibers (Figure 2B). The organization of cells attached to the capsule close to the leak sites is less regular than elsewhere in the lens but no other abnormalities are observed at this stage. Abnormal nuclei or cells seem to

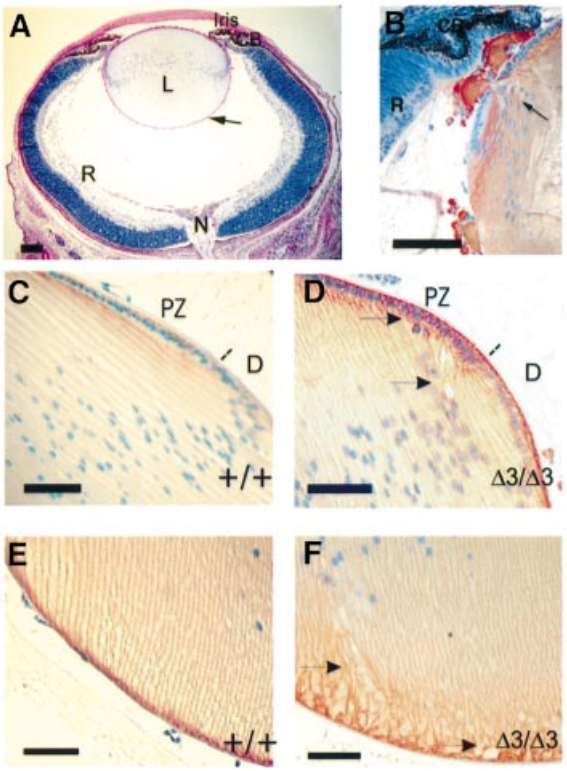

Fig. 2. Early alterations in the eyes of $Hspg2^{\Delta3/\Delta3}$ mutant mice. (**A**) The eye from a newborn $Hspg2^{\Delta3/\Delta3}$ mutant mouse is well developed, but tiny drops of lens material (hardly visible at this magnification) are leaking from the lens (arrow). PAS staining. (**B**) Lateral region of a newborn mutant lens with two leakage sites (one indicated with an arrow) stained with an antibody against γ crystallin. (C–F) Sections of 14-day-old wild-type (**C** and **E**) and $Hspg2^{\Delta3/\Delta3}$ mutant (**D** and **F**) eyes immunostained for N-cadherin, which is localized in the cell membranes (red color). Nuclei are counterstained with hematoxylin. (C and D) Lateral region of the lens. The dotted line indicates the approximate border of the proliferation and differentiation zones. Gaps and irregularities in lens fiber organization are detected in the mutant lens (D). (E and F) The attachment of lens fibers to the lens capsule in the posterior region of the lens is altered in the mutant lens (F). Arrows point to irregularities in the lens fiber organization. Bar: 100 μm in (A), 50 μm in (B–F). CB, ciliary body; D, differentiation zone; L, lens; N, optic nerve; PZ, proliferation zone; R, retina.

depart the epithelial cell layer in the lenses of 14-day-old mice (Figure 2C and D), and irregularities in fiber organization are observed in the posterior region of the lens (Figure 2E and F), being visible in lenses stained for N-cadherin, which is expressed in cell membranes. No alterations in the expression of N-cadherin (Figure 2D–F) or integrin α6 (data not shown) were detected in mutant lenses.

The defects become more obvious with age, the lens fibers losing their organized pattern and liquefying, vacuoles appearing in the anterior and the equatorial region, and extrusion of nucleated cells through the capsule being increased (Figure 3A–D). In addition, single cells are occasionally found within the lens capsule (Figure 3E). In periodic acid–Schiff (PAS)-stained sections the mutant lens capsule appears porous, whereas appearance of the normal lens capsule is uniform and compact (Figure 3B and E). Swelling, liquefaction and degeneration of the fibers continue in the mutants, until finally, at the age of 2–4 months, the lens is composed of

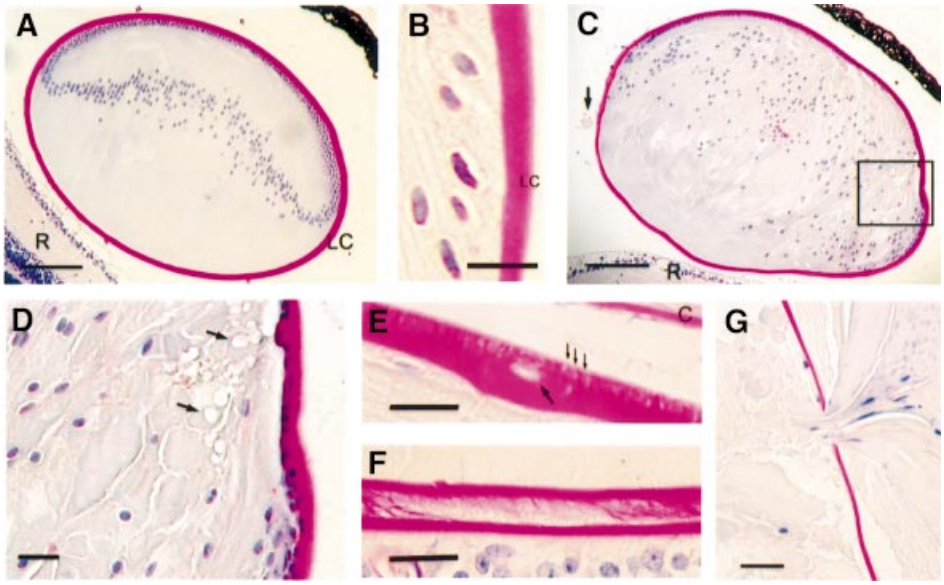

Fig. 3. Degeneration of lenses in the *Hspg2*$^{\Delta3/\Delta3}$ mutant mice. All sections were stained by the PAS method, by which the lens capsule stains red. (**A**) Lens of a 20-day-old wild-type mouse. The lens is contained within the lens capsule and is composed of fiber cells and a monolayer of epithelial cells at the anterior surface. (**B**) The lateral region of the lens in a 6-month-old wild-type mouse. The lens capsule is compact and uniformly stained. (**C** and **D**) Lens of a 20-day-old *Hspg2*$^{\Delta3/\Delta3}$ mutant mouse. The fibers have lost their ordered pattern and have started to liquefy. The lens capsule is wrinkled and drops of lens material (arrow) are visible in the posterior chamber of the eye. (D) Boxed area in (C) in higher magnification. Vacuoles (arrows) are seen in the anterior and equatorial regions. (**E** and **F**) Degeneration of the lens capsule in perlecan$^{\Delta3/\Delta3}$ mutant mice. (E) Anterior region of the lens in a 6-month-old *Hspg2*$^{\Delta3/\Delta3}$ mutant mouse. Small cracks (thin arrows) and a degenerated cell within the lens capsule (faint hematoxylin staining, arrow) are visible. (F) A split capsule in the posterior region of a lens in an 11-month-old *Hspg2*$^{\Delta3/\Delta3}$ mutant mouse. (**G**) Degenerated lens material leaking out of the lens in a 6-month-old *Hspg2*$^{\Delta3/\Delta3}$ mutant mouse. Bar: 100 µm in (A) and (C), 20 µm in (B) and (D–G). C, cornea; LC, lens capsule; R, retina.

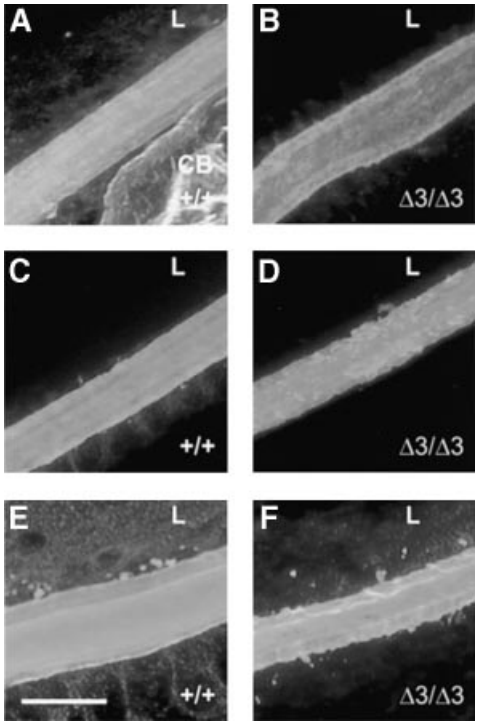

Fig. 4. Immunohistochemical detection of lens capsule components. (**A**, **C** and **E**) Frozen sections of eyes from 14-day-old wild-type and (**B**, **D** and **F**) *Hspg2*$^{\Delta3/\Delta3}$ mutant mice were stained for laminin (A and B), perlecan (C and D) and collagen IV (E and F). All three components are present in the mutant lens, but the lens capsule is more compact in appearance in the wild-type eye. Bar: 20 µm. CB, ciliary body; L, lens.

an amorphous mass of degenerated fibers and only remnants of the epithelial cells and an unorganized bow region are seen. At this stage, the capsule is often wrinkled, of uneven thickness and occasionally split longitudinally, especially in the posterior region where it is thinnest (Figure 3F). Leakage of the lens increases (Figure 3G) and finally it ruptures. No gross alterations have been observed in other parts of the eye.

The major components of the lens capsule, type IV collagen, laminin and perlecan core protein are detected both in *Hspg2*$^{\Delta3/\Delta3}$ mutant and wild-type eyes by immunohistochemistry, but the structure of the lens capsule seems less compact in mutant lenses (Figure 4).

Electron microscopy studies of the lenses from Hspg2$^{\Delta3/\Delta3}$ *mutant and wild-type mice*

Lenses from *Hspg2*$^{\Delta3/\Delta3}$ mutant and wild-type mice of ages 2, 14 and 20 days were analyzed in more detail by transmission electron microscopy. The cytoplasm of the wild-type lens epithelium is pale and ribosomes are mainly located in the rough endoplasmic reticulum (Figure 5A), while by contrast, the epithelial cells in the *Hspg2*$^{\Delta3/\Delta3}$ mutant lenses have a dense cytoplasm, dilated endoplasmic reticulum, large number of free ribosomes and a well defined nucleolus, all signs of high synthetic activity (Figure 5B). As shown previously (Cammarata *et al.*, 1986), the lens capsule in a normal animal has a laminated structure in which repeating filaments are arranged in parallel with the lens surface (Figure 5E). In mutant lenses, the laminated structure is not seen, but the capsule is a homogenous layer of an amorphous appearance (Figure 5F). A difference in organization of the components

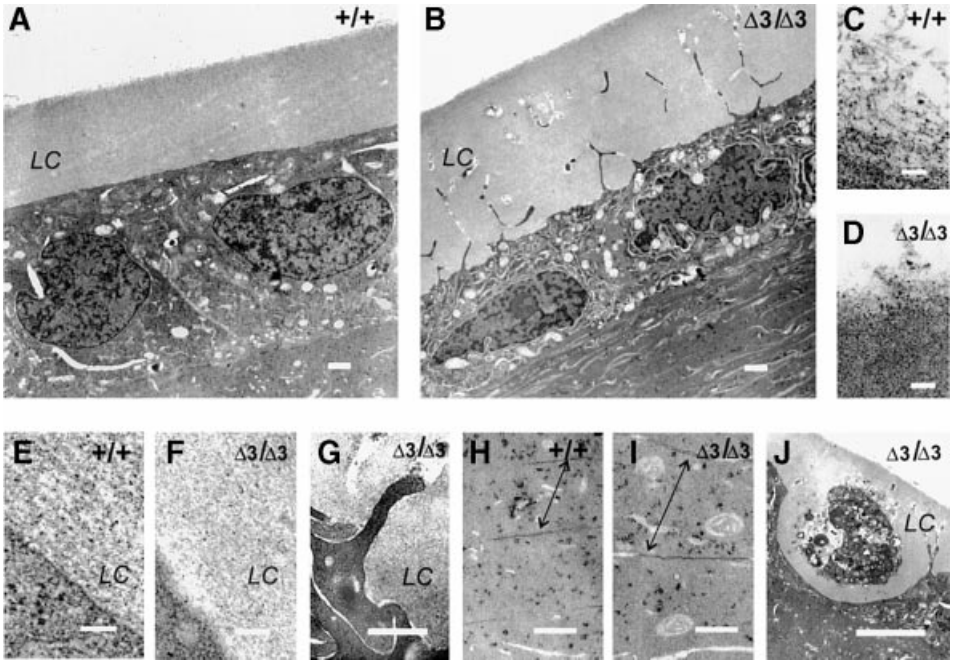

Fig. 5. Transmission electron micrographs of lenses from wild-type and *Hspg2*$^{\Delta3/\Delta3}$ mutant mice. (**A**) Anterior region of a wild-type lens. Lens epithelial cells form a monolayer covered by the lens capsule (LC). (**B**) Lens epithelial cells in the *Hspg2*$^{\Delta3/\Delta3}$ lens have a dilated endoplasmic reticulum, increased number of ribosomes and mitochondria, and filopodia-like protrusions reaching into the lens capsule. Lens fibers below the epithelial cell layer are deteriorating. (**C**) Lens capsule component aggregates on the surface of the wild-type lens capsule have the appearance of a layer of loose filaments. (**D**) Loose amorphous material is seen on the surface of the *Hspg2*$^{\Delta3/\Delta3}$ lens capsule. (**E**) The basolateral surface of the wild-type lens epithelial cell is distinct, and the lens capsule has a layered structure. (**F**) The surface of the *Hspg2*$^{\Delta3/\Delta3}$ lens epithelial cell is fuzzy in appearance and the lens capsule lacks the layered structure. (**G**) The basolateral surface of a *Hspg2*$^{\Delta3/\Delta3}$ lens epithelial cell with a protrusion. A dilated endoplasmic reticulum and loose contact with the lens capsule are discernible. (**H**) The fiber cells in the inner region of the wild-type lens are densely packed. Arrows point to gap junctions. (**I**) The fibers in the *Hspg2*$^{\Delta3/\Delta3}$ lens look swollen, and dense packing is lost. Gap junctions (arrows) are loosened. (**J**) A necrotic epithelial cell within the lens capsule of an *Hspg2*$^{\Delta3/\Delta3}$ lens. Neighbouring epithelial cells have extended protrusions into the lens capsule but have remained in the monolayer. Samples are from 20-day-old mice except (G), which is from a 14-day-old mouse. Bar: 1 μm in (A) and (B), 0.1 μm in (C–F), 0.5 μm in (G–I), 5 μm in (J).

was also recognized on the surface of the lens capsule, where the structure is loosened and the capsule components seem to be shed in the vitreous body, as the loosened material forms long filament-like aggregates in the wild-type lens, whereas the fragments in the *Hspg2*$^{\Delta3/\Delta3}$ mutant lens are short and fluffy (Figure 5C and D).

The contact of the epithelial cells with the lens capsule is altered in the mutants in that the epithelial cells in wild-type lenses have a smooth and well defined basal surface and a distinct border between the cell and the capsule (Figure 5E), whereas in the *Hspg2*$^{\Delta3/\Delta3}$ mutant lenses there seems to be a gap between the capsule and the cell surface, and the cells form filopodia-like protrusions into the lens capsule (Figure 5B, F and G). The projections reach through the capsule, branch and seem to form a three-dimensional mesh. A distinct halo surrounds the protruding parts, which are often degraded, leaving a channel-like empty space within the capsule (Figure 5B and G). In the lenses of young *Hspg2*$^{\Delta3/\Delta3}$ mutant mice, the epithelial cells largely remain connected to each other as a monolayer, as in wild-type lenses, but single necrotic cells seemingly detached from the epithelial layer are occasionally observed (Figure 5J).

Differentiation of the fiber cells is not greatly altered in the lenses of young *Hspg2*$^{\Delta3/\Delta3}$ mutant mice, but early signs of degeneration are visible already at the age of 20 days, when the fibers look swollen, and compact arrangement of fibers is loosened in the mutants (Figure 5H and I).

Analysis of eyes of Col18a1$^{-/-}$ × *Hspg2*$^{\Delta3/\Delta3}$ *mice*

Col18a1$^{-/-}$ × *Hspg2*$^{\Delta3/\Delta3}$ mice were obtained after several generations of crossbreeding. These were viable and had no obvious abnormalities except for the small size of their eyes; the average eye weight of a newborn mouse being 2.1 mg (n = 10), 60% of that of a newborn wild-type mouse, and 77% of that of a *Hspg2*$^{\Delta3/\Delta3}$ mouse (Table I). The ratio remains the same during the first weeks of life so that the average eye weight of a 2-week-old *Col18a1*$^{-/-}$ × *Hspg2*$^{\Delta3/\Delta3}$ mouse is 8.0 mg, 58 % of the eye weight of a wild-type mouse, or 77% of that of a *Hspg2*$^{\Delta3/\Delta3}$ mouse.

Histology of the eyes of neonatal *Col18a1*$^{-/-}$ × *Hspg2*$^{\Delta3/\Delta3}$ mice revealed signs of abnormal development, leakages of cellular material being observed in the anterior region, mainly at locations close to the ciliary body and the iris (Figure 6A). Masses of lens fiber-like cells are found between the lens and the iris and ciliary body in 2-week-old mice (Figure 6B), and abnormal proliferation of the lens epithelial cells and migration towards the ciliary body and iris are observed (Figure 6C and D). The epithelial cells are viable at this stage and deposit large amounts of lens capsule-like extracellular material, but within a few weeks, the external cells will have been degraded and only

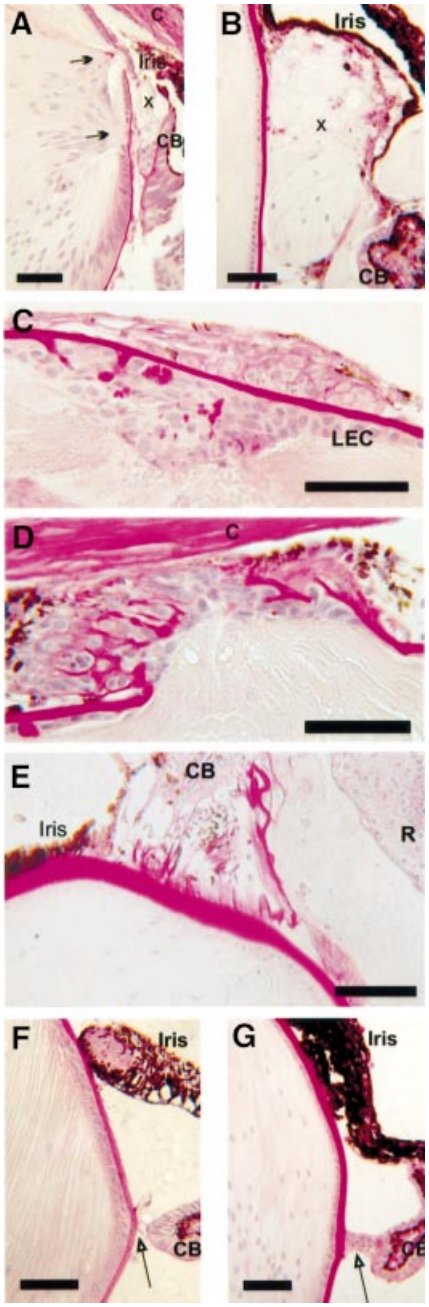

Fig. 6. Abnormal development of lenses in *Col18a1*$^{-/-}$ × *Hspg2*$^{\Delta3/\Delta3}$ mice. (**A**) Section of a newborn eye showing leakage of differentiating fiber cells (arrows) towards the ciliary body and iris. Lens external cytoplasmic material is marked with X. (**B**) Section of the lens of a 2-week-old mouse showing a mass of external lens cells (marked with X) between the disrupted iris and the ciliary body. Degeneration of the iris is typical of *Col18a1*$^{-/-}$ mice. (**C**) The anterior region of a lens in a 2-week-old mouse, with a cluster of proliferating epithelial cells depositing red-stained lens capsule-like extracellular matrix. (**D**) Invasion of lens epithelial cells towards the iris/ciliary body in a lens of a 2-week-old mouse. (**E**) The external cells in the 10-week-old eye have been degraded, and remnants of lens capsule material connect the ciliary body and the deteriorated lens. (**F**) The capillary (arrow) connecting the ciliary body and the lens capsule is still present in the 1-week-old mutant eye. (**G**) The capillary has regressed in the 2-week-old eye, but a bridge-like structure (arrow) has formed between the lens and the ciliary body. The iris is tightly attached to the lens capsule. All sections were stained with PAS method. Bar: 50 μm. C, cornea; CB, ciliary body; LEC, lens epithelial cells; R, retina.

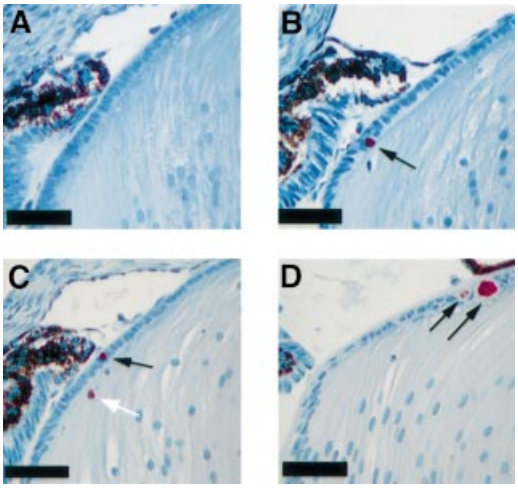

Fig. 7. Detection of apoptotic nuclei in the lens. (A–C) Apoptosis in the eyes of newborn wild-type (**A**), *Hspg2*$^{\Delta3/\Delta3}$ (**B**) and *Col18a1*$^{-/-}$ × *Hspg2*$^{\Delta3/\Delta3}$ mice (**C**) was analyzed by the TUNEL assay. TUNEL-positive nuclei are stained red (arrows). Only nuclei in the epithelial layer (black arrows) were counted for statistical analysis. (**D**) A cluster of apoptotic cells in the epithelial layer of an 11-day-old *Col18a1*$^{-/-}$ × *Hspg2*$^{\Delta3/\Delta3}$ mouse. These clusters were not observed in neonatal samples. Nuclei were counterstained with hematoxylin. Bar: 50 μm.

remnants of extracellular matrix will be left (Figure 6E). In addition to the unorganized mass of cells originating in the lens, more organized, bridge-like structures are observed connecting the ciliary body and the lens, having grown at the site of a former capillary (Figure 6F and G).

Proliferation and apoptosis in newborn lenses

Smaller size of the lenses in newborn mutant mice, when the lens still appears reasonably intact, could be due to decreased proliferation or increased apoptosis. BrdU labeling in newborn mice was used to detect proliferation in the lens epithelial cells. No significant difference was observed in the proliferation rate in the *Hspg2*$^{\Delta3/\Delta3}$ mutant lenses, whereas in the *Col18a1*$^{-/-}$ × *Hspg2*$^{\Delta3/\Delta3}$ double mutants, a significant decrease compared with the wild type was observed (Table II). In double mutant neonatal lenses the epithelial layer does not appear remarkably altered, but abnormal clusters of epithelial cells are detected in lenses of 2-week-old mice (Figure 6C and D).

Apoptosis is rarely detected in the lenses of wild-type mice. Single TUNEL-positive nuclei were observed in the epithelial cell layer in ~25% of sections analyzed. In *Hspg2*$^{\Delta3/\Delta3}$ mutant lenses, apoptotic nuclei were observed in 65% of the sections, and in *Col18a1*$^{-/-}$ × *Hspg2*$^{\Delta3/\Delta3}$ lenses, all sections contained apoptotic nuclei. In both kinds of mutant lenses, the rate of apoptosis in the epithelial cell layer is significantly increased (Figure 7; Table III).

Discussion

In an attempt to understand the biological roles of HS in BMs, in this study, we have genetically modified the perlecan gene in ES cells and generated mice containing perlecan that lacks its three large N-terminal HS side

Table II. Proliferation of epithelial cells in newborn mouse lenses

Genotype	BrdU-positive cells	Total number of cells	%	Number of lenses
Wild type	19 ± 5	165 ± 13	11.6 ± 2.4	10
Hspg2$^{\Delta3/\Delta3}$	15 ± 4	145 ± 19	10.8 ± 3.9	10
Col18a1$^{-/-}$ × *Hspg2*$^{\Delta3/\Delta3}$	13 ± 4	148 ± 14	9.1 ± 2.7[a]	10

[a]$P < 0.001$ versus wild type.

Table III. Apoptosis of epithelial cells in newborn mouse lenses

Genotype	TUNEL-positive cells	Total number of cells	%	Number of lenses
Wild type	0.3 ± 0.6	156 ± 10	0.2 ± 0.4	9
Hspg2$^{\Delta3/\Delta3}$	2 ± 2	151 ± 12	1.1 ± 1.1[a]	10
Col18a1$^{-/-}$ × *Hspg2*$^{\Delta3/\Delta3}$	3 ± 2	150 ± 24	1.9 ± 1.4[a]	10

[a]$P < 0.001$ versus wild type.

chains. Furthermore, since collagen XVIII, another widespread BM component, is also known to carry HS chains (Halfter *et al*., 1998), we bred mice carrying the perlecan mutation with *Col18a1*$^{-/-}$ mice (Fukai *et al*., 2002) to reduce the HS content in BM further.

Targeted depletion of HS chain attachment sites in perlecan

The 45 bp exon 3 of the perlecan gene, which was deleted here by the gene targeting method, codes for a short N-terminal segment with two Ser–Gly–Asp triplets, in which the serine residues are sites for HS side chain attachment (Dolan *et al*., 1997). The code for aspartate in the extreme N-terminal Ser–Gly–Asp triplet is split between exons 2 and 3, and when exon 3 is deleted, the aspartate residue is replaced with valine. The acidic residues preceding the Ser–Gly–Asp sequences at the N-terminus of perlecan are thought to be primary determinants for targeting the serine residues for HS attachment (Dolan *et al*., 1997), and since these residues are not altered in the mutated perlecan, the serine in the Ser–Gly–Val sequence could serve as an HS attachment site. This single Ser–Gly sequence is not likely to be used efficiently as a HS chain attachment site however, firstly, because the acidic residue following the Ser–Gly shown to increase the frequency of glycosaminoglycan chain attachment is abolished, and secondly, because one Ser–Gly sequence is a less likely target for HS attachment than a cluster of Ser–Gly repeats (Dolan *et al*., 1997). The single HS attachment site at the C-terminus of perlecan is unaltered. It is not known how efficiently this latter site is used for HS chain attachment *in vivo*, since only three chains at one end of the molecule were detected in early studies of perlecan purified from tumor material (Paulsson *et al*., 1987), and since the major portion of perlecan isolated from the medium of *Hspg2*$^{\Delta3/\Delta3}$ mutant fibroblasts in our analysis did not contain notable amounts of HS.

Significance of HS chains of perlecan in kidney

The homozygous mutant mice that appeared to express normal amounts of the perlecan core protein were viable and fertile. Importantly, the perlecan mutant mice did not develop proteinuria, demonstrating that the anionic HS side chains of perlecan are not of major importance for the charge barrier or for the filtration of plasma macromolecules in the glomerular BM. It has been suggested that agrin may be the major HSPG in kidney glomerular BM, and therefore the main provider of the negative charge (Groffen *et al*., 1998). The significance of agrin for charge barrier formation in the glomerular BM remains to be tested.

Lens degeneration in *Hspg2*$^{\Delta3/\Delta3}$ mice

The major defect in *Hspg2*$^{\Delta3/\Delta3}$ mice is the early deterioration of the lens. Perlecan is found only in the lens capsule, a specialized, exceptionally thick BM, other major components of which are type IV collagen, laminin and entactin/nidogen. The capsule surrounds the lens vesicle from the time it is formed from the head ectoderm, and both the lens and the capsule continue to grow throughout life. The epithelial cells form a monolayer in the anterior region, their basal surface being attached to the lens capsule, and they divide in the proliferation zone above the lens equator, the progeny of these divisions moving on further and differentiating to lens fibers in the region below the equator. The posterior ends of differentiating fibers migrate beneath the lens capsule to the posterior suture, where they finally detach from the capsule and join to the ends of fiber cells extending from the opposite side of the lens. Coordinated organelle loss occurs after the fiber cells have detached from the lens capsule. The retina and vitreous body are thought to supply the factors necessary for fiber cell differentiation, and distribution of FGF molecules has been shown to be important for the maintenance of normal lens structure (Francis *et al*., 1999; McAvoy *et al*., 1999). In addition, alterations in the lens capsule composition during development and in different regions of the lens may also play a role in cell differentiation (Menko *et al*., 1998).

The *Hspg2*$^{\Delta3/\Delta3}$ mutant lenses maintain their polarity during early development, and lens cell proliferation and differentiation still function normally after birth, albeit focal leaks of cellular material appear in the lateral and posterior regions of the lens. Increased apoptosis is detected in the epithelial cell layer, but the first obvious signs of abnormal development are seen by microscopy in the early differentiation region and in the posterior region of the lens, and degeneration exceeds the proliferation

capacity within 3 weeks. The HS chains of perlecan therefore do not seem to be essential for the development of embryonic lens, even though they are known to bind growth factors important for lens development. The smaller size of the lenses in the newborn mice is probably mainly due to the loss of fiber cells that focally burst out through the weakened lens capsule.

No differences in the thickness or appearance of the lens capsule were observed in light microscopy at the age at which cytoplasmic leakages were first seen, but electron microscopy revealed alterations in its structure. Whereas a lamellar substructure is observed in the wild-type lens capsule, that of the *Hspg2*$^{\Delta3/\Delta3}$ mutants has an appearance of a homogenous mass. The epithelial cells in mutant lenses show high biosynthetic activity, possibly because they try to compensate for the lack of a proper matrix. Even though perlecan is synthesized, the deficiency of HS chains may lead to an altered three-dimensional structure of the lens capsule by interfering with interactions of collagen IV–laminin networks. The assembly of lens capsule is probably different from the assembly of thinner BMs (Timpl and Brown, 1996), which might explain why most BMs are still functional in mutant mice. Altered structural properties are likely to alter the transport of metabolites, nutrients and growth factors, which is likely to contribute to the degeneration of the lens in *Hspg2*$^{\Delta3/\Delta3}$ mice.

The adhesion of lens cells is altered in the *Hspg2*$^{\Delta3/\Delta3}$ mutant lenses, so that both the epithelial and the fiber cells form extensions into and through the lens capsule. The reason for this may be that the capsule does not provide enough support, due to its lack of mechanical strength, and cells seek for proper adhesion substrate by forming the extensions. Cells seemingly invading the lens capsule are occasionally seen in *Hspg2*$^{\Delta3/\Delta3}$ mutant lenses, but these cells are necrotic and their origin is unknown. Formation of cell extensions in *Hspg2*$^{\Delta3/\Delta3}$ lenses may also be an early sign of transdifferentiation due to alterations in lens capsule composition.

Bilateral cataracts were reported in a human fetus suffering from dyssegmental dysplasia, Silverman–Handmaker type, caused by the production of a truncated perlecan core protein (Arikawa-Hirasawa *et al*., 2001). In addition, a dominant congenital cataract Volkmann type has been assigned to chromosome 1p36, close to the perlecan gene locus (Eiberg *et al*., 1995). The expression of the disease is highly variable, ranging from hardly recognizable to dense cataracts. Mature cataracts have not been observed in heterozygous *Hspg2*$^{\Delta3/+}$ mice, but mild opacities typical to Volkmann patients may have been unnoticed, and will be studied by slit lamp examinations in a separate study.

Early abnormalities in the lenses of *Col18a1*$^{-/-}$ × *Hspg2*$^{\Delta3/\Delta3}$ mice

The lenses in *Col18a1*$^{-/-}$ mice develop normally, although delayed regression of blood vessels along the surface of the retina in the vitreous body and abnormal outgrowth of retinal vessels are observed (Fukai *et al*., 2002). In *Col18a1*$^{-/-}$ × *Hspg2*$^{\Delta3/\Delta3}$ mice, however, lens degeneration is accelerated relative to that in *Hspg2*$^{\Delta3/\Delta3}$ mice, and additional defects are observed. The first signs of abnormal development are already detectable in neonatal mice in that leakages of cells are detected in the anterior region of the lens. In *Hspg2*$^{\Delta3/\Delta3}$ mice, leakages are observed in a more posterior region and are less severe. Furthermore, in *Col18a1*$^{-/-}$ × *Hspg2*$^{\Delta3/\Delta3}$ lenses, epithelial cells migrate focally outwards, proliferate markedly and remain external for several weeks. These results imply that HS chains of other capsule components, mainly collagen XVIII, can partly substitute for those of perlecan. The lens capsule is functional until late embryogenesis in both kinds of mutant mice, which indicates that its functions change during development. Apoptosis of lens epithelial cells is significantly increased in both types of mutants already at the neonatal stage. Lens epithelium-derived growth factor (LEDGF), is expressed strongly in lens epithelial cells. It is actually a survival factor that negatively regulates apoptosis. Heparin stabilizes LEDGF and protects it from deactivation (Shinohara *et al*., 2002). Depletion of HSs can therefore lead to loss of LEDGF activity and result in increased apoptosis.

Our results suggest that the major function of the lens capsule promoted by the HS chains in the postnatal eye is to serve as a barrier that insulates the lens from its environment and regulates its interactions. This function becomes essential when the capillaries around the lens (tunica vasculosa lentis) regress after birth. When the barrier function is lost, cells can traverse the lens capsule and signals from other regions of the eye disturb the strictly organized proliferation and migration.

Materials and methods

Generation of mice with an altered perlecan gene

A 650 bp cDNA fragment coding for the N-terminal region of the murine perlecan gene (*Hspg2*) was amplified from poly(A) RNA isolated from F9, F10 and PYS cell lines, and used as a probe to screen the 129SV mouse genomic λ phage library (Stratagene). The genomic clone obtained was used to clone the targeting construct. It contains 2 and 5.5 kb genomic arms with a 130 bp *Kpn*I–*Bam*HI fragment containing exon 3 deleted, and the PGK-*neo* marker gene inserted into intron 2 (Figure 1A). The *Not*I-linearized construct was electroporated into E14 ES cells. Cells were selected in a medium containing G418 and resistant cell clones were picked. Electroporation and selection were carried out at the transgenic mouse core facility at Karolinska Institutet. Genomic DNA from ES cell clones was digested with *Eco*RI, and Southern blots were hybridized with an external 0.5 kb *Pst*I–*Bam*HI fragment containing exons 4 and 5 (Figure 1B). Clones in which homologous recombination was detected were expanded and injected into C57BL/6 blastocysts. Two mouse lines, originating from clones 2B and 3C, were obtained by mating the chimeras with C57BL/6 mice. From the 3C clone, both a male and a female chimera transmitted the coat color into their offspring when mated with C57BL/6 mice, but only the female chimera transmitted the mutated allele into the offspring. Homozygous mice were obtained by cross-breeding the heterozygotes. The mutation was backcrossed into the C57BL/6 background for 12 generations.

RT–PCR

Poly(A) RNA was isolated from F9, F10 and PYS cells by standard methods using oligo-dT cellulose. Total RNA was isolated from E16 embryos using Trizol (Gibco), and poly(A) RNA was isolated from primary fibroblasts using the Quick Prep Micro mRNA Purification Kit (Amersham Pharmacia). For RT–PCR, primer PC-1 5′-CTTTCC-CTCCCTGAGGACAC from exon 2 and primer PC-3 5′-CACAGCA-GGTGTCGAGGAGC from exon 7 were used. The amplified product is 650 bp from the wild-type allele and 605 bp from the *Hspg2*$^{\Delta3/\Delta3}$ mutant allele, in which exon 3 is deleted.

Cell cultures

Primary fibroblasts were cultured from skin of wild-type and *Hspg2*$^{\Delta3/\Delta3}$ mutant mice. A segment of the skin was excised and diced, incubated in

0.1% trypsin at 37°C for 1 h and plated in tissue culture dishes. Fibroblasts were grown in RPMI or DMEM medium containing 10% FCS.

Isolation and analysis of perlecan

Proteoglycans were isolated from the culture media of confluent primary fibroblasts. Briefly, urea was added to the medium to a final concentration of 7 M and the medium was then applied to a DEAE–Sepharose column in 7 M urea, 50 mM Tris–HCl pH 7.4, 1% CHAPS and protease inhibitors. The bound material was washed with 10 column volumes of 0.185 M NaCl and eluted with 1.5 M NaCl in the same solution and precipitated with ethanol.

Proteoglycan-enriched DEAE–Sepharose fractions were treated with heparitinase alone, chondroitinase alone and heparitinase plus chondroitinase, and immunoblot analysis was carried out as described previously (Kato *et al*., 1987) with minor modifications. The digests were precipitated with ethanol and redissolved in SDS sample buffer. After heating at 100°C, the digests were subjected to SDS–PAGE under unreduced conditions. The proteins separated in a 5% polyacrylamide gel were transferred to a nitrocellulose membrane and the membrane was soaked with 10% non-fat milk and 1% BSA and then incubated with an affinity-purified rat anti-mouse perlecan antibody (HK-102; Seikagaku) for 2 h at room temperature. After washing, the membrane was incubated with ^{125}I-labeled sheep anti-rat immunoglobulins (Amersham Pharmacia Biotech). The protein bands were then visualized by autoradiography.

Histology and immunohistochemistry

Mice were killed by cervical dislocation or by CO_2 asphyxiation. Tissues were collected and fixed in neutral formalin and processed for paraffin sectioning. Sections of 3–8 μm were stained with hematoxylin–eosin or PAS method, or stained with N-cadherin antibodies (provided by Dr M.Wheelock and Dr K.Johnson, University of Toledo, Ohio) with Histomouse SP bulk kit (Zymed Laboratories), or with rabbit antisera against bovine γ crystallin (provided by Dr S.J.Zigler, NEI, Bethesda, MD) and HRP-conjugated goat anti-rabbit IgG (Promega). The substrate used was 3-amino-9-ethyl carbazole (AEC). Nuclei were counterstained with hematoxylin.

Alternatively, tissue samples were snap-frozen in isopentane cooled in liquid nitrogen. Frozen sections of 12–14 μm were stained following standard procedures. The primary antibodies used were monoclonal rat anti-laminin B2 chain (γ1), monoclonal rat anti-HS proteoglycan and polyclonal rabbit anti-mouse collagen IV (Chemicon), and the secondary antibodies Cy3-conjugated goat anti-rat IgG or goat anti-rabbit IgG (Jackson Immuno Research Laboratories Inc.), depending on the primary antibody, and visualized under UV light.

Detection of proliferation and apoptosis

BrdU (125 μg) in 25 μl saline were injected into newborn pups that were sacrificed 2 h after injection, and their eyes were processed for paraffin sectioning. Midsagittal 5 μm sections were treated with proteinase K and 0.2 M HCl and stained using 5-bromo-2′deoxy-uridine Labeling and Detection Kit II (Roche Diagnostics) and Alkaline Phosphatase Substrate Kit I (Vector Laboratories) as a substrate and hematoxylin as a counterstain. Digital images of sections were captured under light microscopy to count the total number of nuclei, and under UV light to visualize the nuclei that had incorporated BrdU. Ten lenses of each genotype were analyzed, and nuclei in four sections of each lens were counted. Statistical analysis was made by Student's two-tailed *t*-test.

For the TUNEL assay, midsagittal 5 μm paraffin sections of neonatal mouse eyes were stained using the ApopTag Peroxidase *In Situ* Apoptosis Detection Kit (Intergen Company) and AEC as a substrate. Nuclei were counterstained with hematoxylin. Ten lenses of mutant newborn pups and nine lenses of wild-type pups were subjected to the analysis, and nuclei in four sections of each lens were counted. Statistical analysis was made by Student's one-tailed *t*-test.

Protein analysis of urine

Urine samples were collected from 6- to 8-week-old mice (both male and female) in a metabolic cage, or with a syringe from the bladder of the male mice more than 12 months old immediately after killing. Samples (5 μl) were separated in a 10% SDS–PAGE gel and silver-stained using the Silver Stain Plus Kit (Bio-Rad).

Electron microscopy

Eyes were collected from 2, 14 and 20-day-old and 8-month-old mice, and kidney samples from 12- to 18-month-old mice, and fixed in 2.5% glutaraldehyde in 0.1 M phosphate buffer, postfixed in 1% osmiumtetroxide, dehydrated in acetone and embedded in Epon LX112. Thin sections were cut with a Reichert Ultracut ultramicrotome and examined in a Philips CM100 transmission electron microscope.

Breeding of *Col18a1*$^{-/-}$ × *Hspg2*$^{\Delta 3/\Delta 3}$ mice

The generation of *Col18a1*$^{-/-}$ mice has been described previously (Fukai *et al*., 2002). The mutation had been backcrossed to C57BL/6 background for 14 generations before breeding with *Hspg2*$^{\Delta 3/\Delta 3}$ mice, backcrossed to C57BL/6 for 12 generations.

Acknowledgements

We thank Ulla Mikkonen, Miia Rahkola and Johanna Räisänen for expert technical assistance. We are grateful to Dr Margaret Wheelock and Dr Keith Johnson, University of Toledo, Ohio, for the N-cadherin antibodies, and to Dr Samuel Zigler, National Eye Institute, Bethesda, MD, for crystallin antibodies. This work was supported by funding from the Swedish Medical Research Council and the Novo Nordisk Foundation.

References

Arikawa-Hirasawa,E., Watanabe,H., Takami,H., Hassell,J.R. and Yamada,Y. (1999) Perlecan is essential for cartilage and cephalic development. *Nat. Genet.*, **23**, 354–358.

Arikawa-Hirasawa,E., Wilcox,W.R., Le,A.H., Silverman,N., Govindraj,P., Hassell,J.R. and Yamada,Y. (2001) Dyssegmental dysplasia, Silverman–Handmaker type, is caused by functional null mutations of the perlecan gene. *Nat. Genet.*, **27**, 431–434.

Aviezer,D., Hecht,D., Safran,M., Elsinger,M., David,G. and Yayon,A. (1994) Perlecan, basal lamina proteoglycan, promotes basic fibroblast growth factor-receptor binding, mitogenesis, and angiogenesis. *Cell*, **79**, 1005–1013.

Battaglia,C., Mayer,U., Aumailley,M. and Timpl,R. (1992) Basement membrane heparan sulfate proteoglycan binds to laminin by its heparan sulfate chains and to nidogen by sites in the protein core. *Eur. J. Biochem.*, **208**, 359–366.

Battaglia,C., Aumailley,M., Mann,K., Mayer,U. and Timpl,R. (1993) Structural basis of β1 integrin-mediated cell adhesion to a large heparan sulfate proteoglycan from basement membranes. *Eur. J. Cell Biol.*, **61**, 92–99.

Cammarata,P., Cantu-Crouch,D., Oakford,L. and Morrill,A. (1986) Macromolecular organization of bovine lens capsule. *Tissue Cell*, **18**, 83–97.

Cohen,I.R., Grässel,S., Murdoch,A.D. and Iozzo,R. (1993) Structural characterization of the complete human perlecan gene and its promoter. *Proc. Natl Acad. Sci. USA*., **90**, 10404–10408.

Costell,M., Gustafsson,E., Aszódi,A., Mörgelin,M., Bloch,W., Hunziker,E., Addicks,K., Timpl,R. and Fässler,R. (1999) Perlecan maintains the integrity of cartilage and some basement membranes. *J. Cell Biol.*, **147**, 1109–1122.

Dolan,M., Horchar,T., Rigatti,B. and Hassell,J.R. (1997) Identification of sites in domain I of perlecan that regulate heparan sulfate synthesis. *J. Biol. Chem.*, **272**, 4316–4322.

Eiberg,H., Meldgaard Lund,A., Warburg,M. and Rosenberg,T. (1995) Assignment of congenital cataract Volkmann type (CCV) to chromosome 1p36. *Hum. Genet.*, **96**, 33–38.

Francis,P.J., Berry,V., Moore,A.T. and Bhattacharya,S. (1999) Lens biology: development and human cataractogenesis. *Trends Genet.*, **15**, 191–196.

Friedrich,M.V., Göhring,W., Mörgelin,M., Brancaccio,A., David,G. and Timpl,R. (1999) Structural basis of glycosaminoglycan modification and of heterotypic interactions of perlecan domain V. *J. Mol. Biol.*, **294**, 259–270.

Fukai,N. *et al.* (2002) Lack of collagen XVIII/endostatin results in eye abnormalities. *EMBO J.*, **21**, 1535–1544.

Groffen,A.J. *et al.* (1998) Agrin is a major heparan sulfate proteoglycan in the glomerular basement membrane. *J. Histochem. Cytochem.*, **46**, 19–27.

Halfter,W., Dong,S., Schurer,B. and Cole,G.J. (1998) Collagen XVIII is a basement membrane heparan sulfate proteoglycan. *J. Biol. Chem.*, **273**, 25404–25412.

Hassell,J.R., Robey,P.G., Barrach,H.J., Wilczek,J., Rennard,S.I. and Martin,G.R. (1980) Isolation of a heparan sulfate-containing proteoglycan from basement membrane. *Proc. Natl Acad. Sci. USA*, **77**, 4494–4498.

Hayashi,K., Madri,J.A. and Yurchenco,P. (1992) Endothelial cells interact with the core protein of basement membrane perlecan through β1 and β3 integrins: an adhesion modulated by glycosaminoglycan. *J. Cell Biol.*, **119**, 945–959.

Iozzo,R. (1998) Matrix proteoglycans: from molecular design to cellular function. *Annu. Rev. Biochem.*, **67**, 609–652.

Iozzo,R., Cohen,I.R., Grässel,S. and Murdoch,A.D. (1994) The biology of perlecan: the multifaceted heparan sulfate proteoglycan of basement membranes and pericellular matrices. *Biochem. J.*, **302**, 625–639.

Kallunki,P. and Tryggvason,K. (1992) Human basement membrane heparan sulfate proteoglycan core protein: a 467-kD protein containing multiple domains resembling elements of the low density lipoprotein receptor, laminin, neural cell adhesion molecules, and epidermal growth factor. *J. Cell Biol.*, **116**, 559–571.

Kanwar,Y.S. and Farquahar,M.G. (1979) Presence of heparan sulfate in the glomerular basement membrane. *Proc. Natl Acad. Sci. USA.*, **76**, 1303–1307.

Kato,M., Koike,Y., Ito,S., Suzuki,S. and Kimata,K. (1987) Multiple forms of heparan sulfate proteoglycans in the Engelbreth–Holm–Swann tumor: the occurence of high density forms bearing both heparan sulfate and dermatan sulfate side chains. *J. Biol. Chem.*, **262**, 7180–7188.

Lundmark,K., Tran,P.K., Kinsella,M.G., Clowes,A.W., Wight,T.N. and Hedin,U. (2001) Perlecan inhibits smooth muscle cell adhesion to fibronectin: role of heparan sulfate. *J. Cell Physiol.*, **188**, 67–74.

McAvoy,J.W., Chamberlain,C.G., de Iongh,R.U., Hales,A.M. and Lovicu,F.J. (1999) Lens development. *Eye*, **13**, 425–437.

Menko,S., Philip,N., Veneziale,B. and Walker,J. (1998) Integrins and development: how might these receptors regulate differentiation of the lens. *Ann. N. Y. Acad. Sci.*, **842**, 36–41.

Noonan,D.M., Fullet,A., Valente,P., Cai,S., Horigan,E., Sasaki,M., Yamada,Y. and Hassell,J.R. (1991) The complete sequence of perlecan, a basement membrane heparan sulfate proteoglycan, reveals extensive similarity with laminin A chain, low density lipoprotein-receptor, and the neural cell adhesion molecule. *J. Biol. Chem.*, **266**, 22939–22947.

Paulsson,M., Yurchenco,P.D., Ruben,G.C., Engel,J. and Timpl,R. (1987) Structure of low density heparan sulfate proteglycan isolated from a mouse tumor basement membrane. *J. Mol. Biol.*, **197**, 297–313.

Shinohara,T., Singh,D.P. and Fatma,N. (2002) LEDGF, a survival factor, activates stress-related genes. *Prog. Retin. Eye Res.*, **21**, 341–358.

Tapanadechopone,P., Hassell,J.R., Rigatti,B. and Couchman,J. (1999) Localization of glycosaminoglycan substitution sites on domain V of mouse perlecan. *Biochem. Biophys. Res. Commun.*, **265**, 680–690.

Timpl,R. and Brown,J.C. (1996) Supramolecular assembly of basement membranes. *BioEssays*, **18**, 123–132.

Tsen,G., Halfter,W., Kroger,S. and Cole,G.J. (1995) Agrin is a heparan sulfate proteoglycan. *J. Biol. Chem.*, **270**, 3392–3399.

Whitelock,J.M., Murdoch,A.D., Iozzo,R.V. and Underwood,P.A. (1996) The degradation of human endothelial cell-derived perlecan and release of bound basic fibroblast growth factor by stromelysin, collagenase, plasmin, and heparanases. *J. Biol. Chem.*, **271**, 10079–10086.

Yurchenco,P., Cheng,Y.S. and Ruben,G.C. (1987) Self-assembly of a high molecular weight basement membrane heparan sulfate proteoglycan into dimers and oligomers. *J. Biol. Chem.*, **262**, 17668–17676.

Received July 18, 2002; revised November 12, 2002; accepted November 14, 2002